Chapter 1

Introduction

The lipid bilayer is the structural basis of all biological membranes [1]. It is a two dimensional fluid in which the membrane proteins and other embedded molecules are free to diffuse. Recent studies have indicated that the distribution of molecules in cell membranes is not random, and microdomains, called lipid rafts, rich in cholesterol are present in them. These rafts are also enriched in certain types of lipids and lipid anchored proteins, and their formation is often considered to be analogous to a phase separation in the lipid bilayer. These membrane rafts are believed to play an important role in many cellular processes, such as protein trafficking and signal transduction. The cell membrane is a very complex system due to the wide variety of lipids and proteins present in it, as well as the various active processes taking place at the cell surface. Therefore, it is important to establish the structure and phase behaviour of model membranes containing cholesterol, in order to understand the formation of rafts in cell membranes.

The present thesis deals with x-ray diffraction and fluorescence microscopy studies on binary and ternary lipid-cholesterol membranes. Section 1.1 describes the hydrophobic effect and self assembly of amphiphilic molecules. The phase behaviour of lipid–water systems is described in section 1.2. Earlier studies of the influence of cholesterol on lipid membranes are summarized in sections 1.3 and section 1.4 gives a brief introduction to membrane rafts.

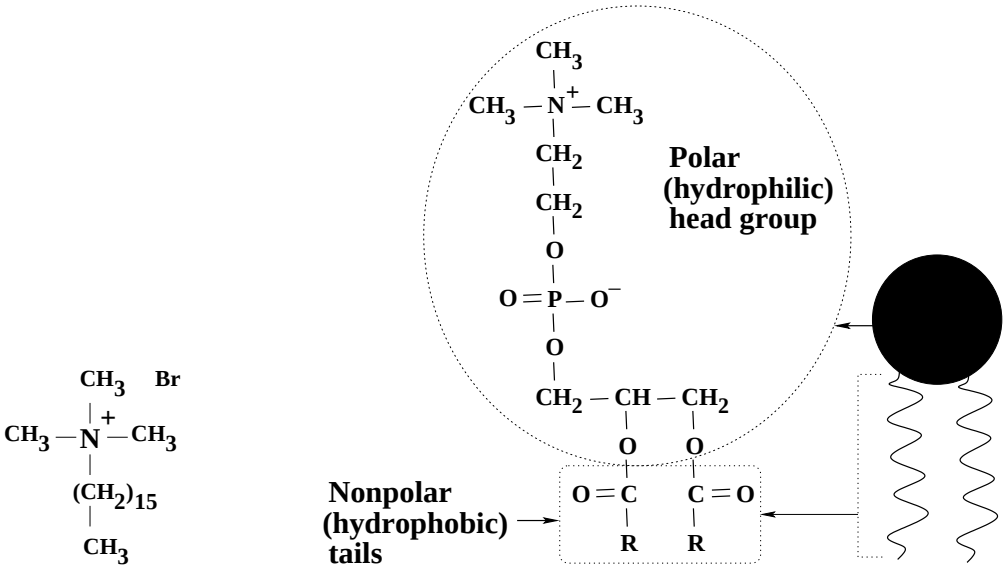

(a) CTAB (b) DPPC (R = $(CH_2)_{14}$–CH_3)

Figure 1.1: Chemical structure of CTAB (a) and DPPC (b).

1.1 Self assembly of amphiphilic molecules

Amphiphilic molecules, such as surfactants, consist of a polar (hydrophilic) part, usually called the head group, attached to a nonpolar (hydrophobic) part consisting of one or more hydrocarbon chains (Fig. 1.1). Lipids are amphiphilic molecules of biological origin. An example of a synthetic surfactant molecule is cetyltrimethylammonium bromide (CTAB) (Fig. 1.1 a) and dipalmitoyl phosphatidylcholine (DPPC) (Fig. 1.1 b) is a lipid found in biomembranes.

Water is a polar solvent and forms a hydrogen bonded network. Typically ~ 3-3.5 hydrogen bonds are associated with each molecule in bulk water at ambient temperature. Strength of this bond is ~ 40 kJ/mol, which is more than that of van der Waals "bond" (~ 1 kJ/mol), but much less than that of the covalent or ionic bonds (~ 500 kJ/mol). Nonpolar molecules are incapable of forming hydrogen bonds with water molecules. Therefore, when water molecules are in contact with a nonpolar molecule they reorient around it so as to retain the hydrogen bonded network. The number of hydrogen bonds per molecule around the nonpolar solute is often more than that in bulk water, resulting in a more ordered state. This is entropically unfavourable. Therefore, nonpolar molecules are highly insoluble in water. The

immiscibility of nonpolar or inert substances in water is known as the hydrophobic effect [2]. This is entirely an entropic effect. Hydrophobic effect plays a vital role in many phenomena, such as protein folding. Another such phenomenon, namely self assembly of amphiphilic molecules, is discussed below.

At sufficiently low concentrations, amphiphilic molecules form a monolayer at the air–water interface in order to minimize the contact between their chains and water. On increasing the concentration of amphiphiles, they aggregate above a critical micellar concentration (CMC) via spontaneous self association. Self assembly of amphiphiles can lead to various structures like micelles and vesicles shown in Fig. 1.2 a, b and c. Below, we describe the thermodynamic principles of self assembly of amphiphiles and then the factors determining the equilibrium shapes and sizes of these aggregates.

Consider a dilute solution of amphiphiles, where aggregates of various sizes are in equilibrium. Their sizes can be described in terms of aggregation number N, which is the number of amphiphiles in an aggregate (N=1 corresponds to monomers). Equilibrium thermodynamics demands that the chemical potential μ of an amphiphile has to be the same in all aggregates, i.e, $\mu_1 = \mu_2 = \mu_3 = ... = \mu_N$. It can be written as

$$\mu_N = \mu_N^0 + \frac{kT}{N} log(\frac{X_N}{N}) = Constant \tag{1.1}$$

μ_N^0 is the reference chemical potential corresponding to the interaction free energy per molecule due to the presence of all other molecules within the aggregate of aggregation number N, and X_N is the total concentration of amphiphiles in aggregates of size N. The second term in equation 1.1 arises from the entropy of mixing. We assume the total concentration (X) of the system is small, i.e,

$$X = \sum_{N=1}^{\infty} X_N \ll 1 \tag{1.2}$$

From $\mu_N = \mu_1$, we get

$$X_N = N[X_1 exp\{(\mu_1^0 - \mu_N^0)/kT\}]^N = N(X_1 e^{\alpha})^N \tag{1.3}$$

where $\alpha = \frac{\mu_1^0 - \mu_N^0}{kT}$. The formation of aggregates of size N is possible if $\mu_N^0 < \mu_1^0$. When $X_1 \ll 1$, $X_1 e^{\alpha} < 1$ and we must have $X_N \ll X_1$ for sufficiently low monomer concentrations. Then,

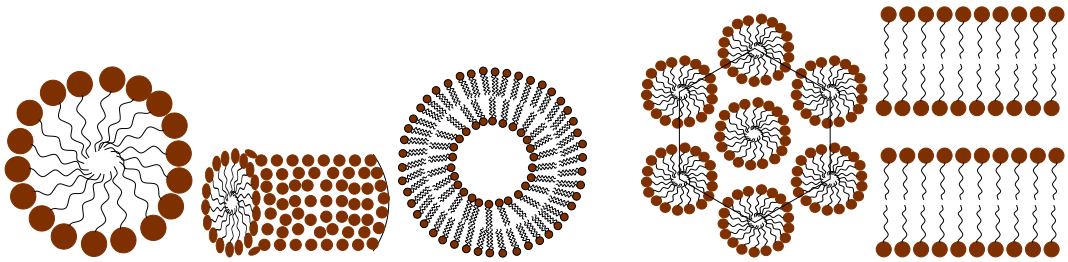

Figure 1.2: Self assembled structures of amphiphilic molecules above CMC. In all these structures hydrophilic part is in contact with water and hydrophobic part is shielded from water. (a) Spherical micelle ; (b) cylindrical micelle ; (c) vesicle ; (d) hexagonal phase made up of cylindrical micelles; (e) lamellar phase.

$X \approx X_1$ and the isolated monomers in solution will be the favoured state. As X_1 is increased $X_1 e^{\alpha}$ approaches unity. Since $X_N < 1$, X_1 cannot exceed a value of the order of $e^{-\alpha}$. Therefore, the monomer concentration should saturate at a value $\sim e^{-\alpha}$, beyond which aggregates are formed. This concentration is known as critical micellar concentration (CMC). It is given by

$$CMC = (X)_c \approx (X_1)_c \approx e^{-(\mu_1^0 - \mu_N^0)/kT}. \tag{1.4}$$

Typical CMC of a surfactant, such as CTAB, is $\sim 10^{-3}$ M and that of a lipid, such as DPPC, is $\sim 10^{-12}$ M. The much lower CMC of DPPC is due to the presence of two long hydrocarbon chains.

In a dilute aqueous solution of surfactants, spherical micelles form. On increasing the concentration, the micellar shape usually changes. For example, CTAB forms spherical micelles just above CMC. A sphere to rod transition of the micellar shape occurs on increasing the concentration. Lipids, such as DPPC, only form bilayers above CMC. Since the edges of the bilayers are in contact with water, these bilayers form a closed shell due to the energetic cost of the hydrophobic edges that are exposed to water. These closed bilayers are known as vesicles (Fig. 1.2 c). The equilibrium size and shape of the aggregates are determined by the forces between the amphiphiles within the aggregates, inter aggregate forces, and the geometry of the molecules. Efficient packing of molecules within the aggregate depends on the geometric shape of an amphiphile. It has been established that relative sizes of the head group and hydrocarbon chain or chains determine the shape of the aggregate structure

[2]. For example, the single chained amphiphile CTAB forms spherical micelles, whereas its double chained lipid analog only forms bilayers. However, the aggregate structure can change on changing the temperature and solution conditions (ionic strength and concentration of amphiphiles) [2, 3].

In a concentrated solution these aggregates form a variety of liquid crystalline phases, characterized by long-range orientational ordering of the aggregates. The most common of these are the hexagonal and lamellar phases. The hexagonal phase consists of cylindrical micelles arranged on a two dimensional hexagonal lattice (Fig. 1.2 d) and the lamellar phase consists of a stack of bilayers separated by water (Fig. 1.2 e).

1.2 Phase transitions of lipid bilayers

Lipids are the main constituents of plasma membranes and they form the structural basis of these membranes. A lipid molecule can have one or more hydrocarbon chains. Although there are a variety of lipids present in the cell membranes, phospholipids and sphingolipids are the most abundant.

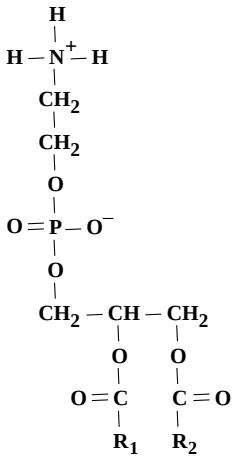

(a) PE

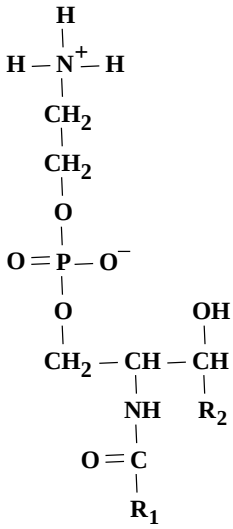

(b) Sphingomyelin

Figure 1.3: Chemical structure of phosphatidylethanolamine (PE) (a) and sphingomyelin (b). R_1 and R_2 represent $(CH_2)_n$-CH_3 units of the chains.

Phospholipids are classified into several groups depending on the chemical structure of

Table 1.1: List of lipids used in the studies presented in this thesis. All these lipids have two identical chains. The numbers of carbon atoms in the chains and the number of double bonds are also given. The position of the double bond along the chain (starting from the ester group) and its conformation are indicated in the bracket. T_m is the main transition temperature.

Lipids	Abbreviation	Lipid chains	T_m (°C)
Dimyristoyl phosphatidylcholine	DMPC	14:0/14:0	24
Dipalmitoyl phosphatidylcholine	DPPC	16:0/16:0	42
Dioleoyl phosphatidylcholine	DOPC	18:1/18:1(cis-9)	-18.3
Dilauryl phosphatidylethanolamine	DLPE	12:0/12:0	30
Sphingomyelin (from bovine brain)	-	Distribution of chains	40

the head group. Phosphatidylcholines (PCs), phosphatidylethanolamines (PEs) and phosphatidylserines (PSs) are common phospholipids found in the plasma membranes. Typical structure of a PC molecule is shown in Fig. 1.1 b and that of PE is shown in Fig. 1.3 a. Among sphingolipids, sphingomyelin (Fig. 1.3 b), sphingosine and gangliosides are the major classes. These lipids may be charged or neutral. Neutral lipids which possess dipole moments in aqueous solution are known as zwitterionic.

Self assembly of lipids in an aqueous solution leads to the formation of lamellar phases, consisting of a stack of bilayers separated by water. Depending upon the nature of the head group and temperature they exhibit a variety of lamellar phases [4].

Lipids form a fluid phase at high temperatures, whose structure is shown in Fig. 1.4. In this phase, known as L_α phase, the hydrocarbon chains are completely molten and disordered. Typical lateral diffusion constant and bilayer bending modulus in this phase are $\sim 10^{-11}\ m^2 s^{-1}$ and $\sim 10^{-19}$ J ($\sim$ 10 - 20 kT), respectively. Positional correlations in the plane of bilayer are short range like in a liquid. Diffraction pattern of the L_α phase, shown in Fig. 1.5, consists of a few lamellar reflections. The higher order reflections are generally smeared out due to the thermal undulations of bilayers. Water can penetrate deep into the membranes due to the flexible bilayer in this phase. The temperature (T_m) above which the L_α phase occurs is known as the main transition temperature and is different for different lipids. T_m is dependent on the number of carbon atoms, number of double bonds in the hydrocarbon chain, and also

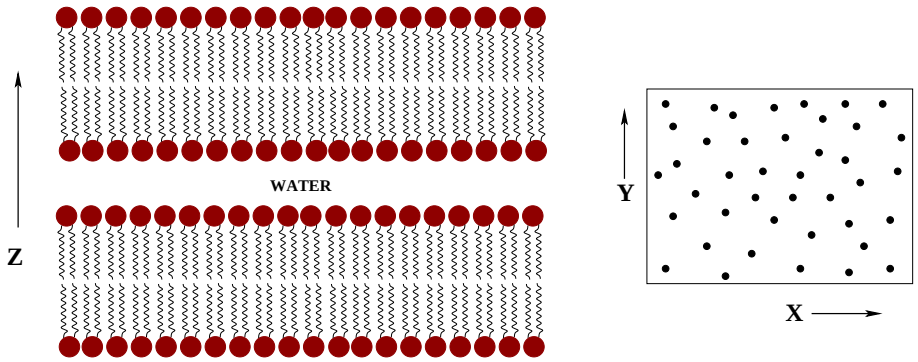

Figure 1.4: Schematic representation of the L_α phase. Dots in the figure depict the position of the chains of the lipid molecules in the plane of the bilayer.

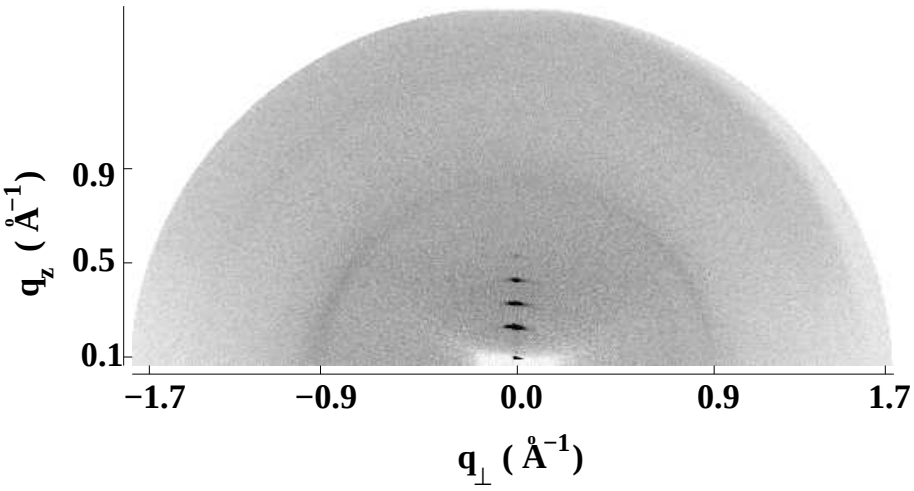

Figure 1.5: Diffraction pattern of the L_α phase

on the nature of the head group. T_m of a few lipids are listed in table 1.1 [5]. The position of the double bond and its conformational (*cis*/*trans*) state in the hydrocarbon chain change the transition temperature drastically. For example, in the case of DOPC, T_m reduces from 41 to -18.3°C as the position of the double bond changes from the 2^{nd} to the 9^{th} carbon atom (starting from the ester group) in the chain. At a given position of the double bond, *cis* configuration has a considerably lower transition temperature compared to *trans*. Typical enthalpy change during the main transition is about 5-10 kcal/mol for phospholipids [5].

On decreasing temperature, the L_α phase transforms into a gel phase, where hydrocarbon chains are predominantly in the fully stretched all *trans* conformation. Chains form a quasi hexagonal lattice in the plane of bilayers. There are two types of gel phases found in lipids. The L_β phase is exhibited by lipids, such as PE, where hydrocarbon chains are parallel to the

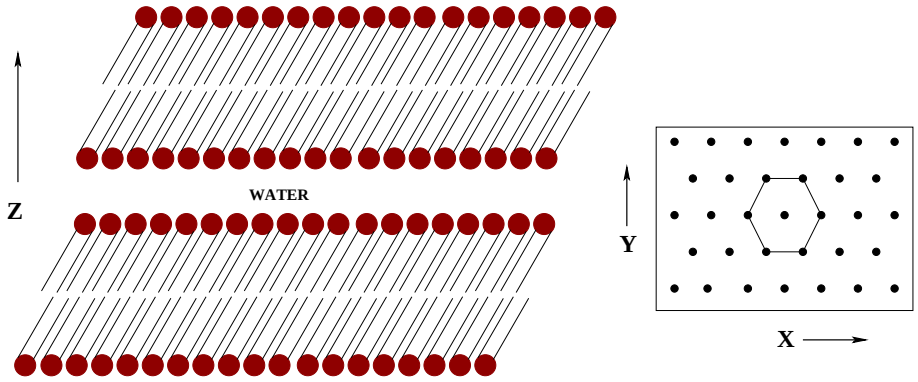

Figure 1.6: Schematic representation of the $L_{\beta'}$ phase.

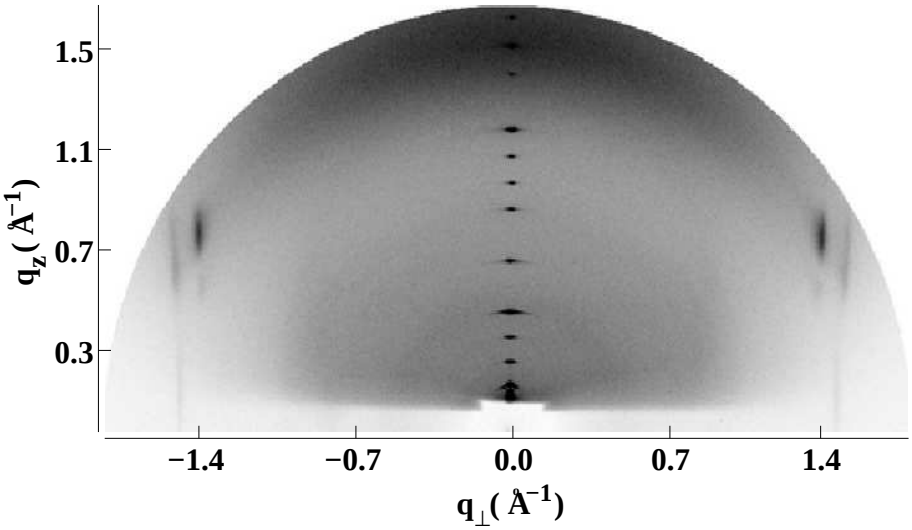

Figure 1.7: Diffraction pattern of the $L_{\beta'}$ phase.

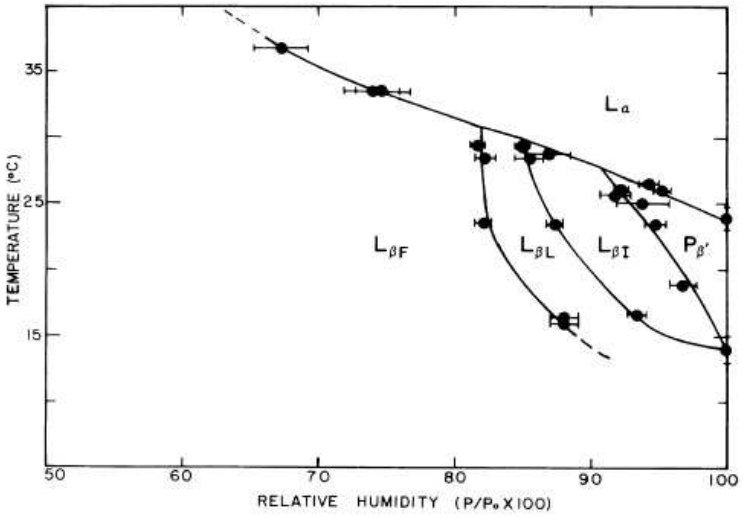

Figure 1.8: Phase diagram of the DMPC-water system [6].

bilayer normal (zero tilt). Some lipids with larger head groups, such as PC, exhibit the $L_{\beta'}$ phase where chains are tilted with respect to bilayer normal as shown in Fig. 1.6. Typical diffraction pattern of such a gel phase is shown in Fig. 1.7. Large number of lamellar reflections along q_z implies very rigid bilayers in this phase. Wide angle reflections at $q_z \neq 0$ suggest the tilt of the hydrocarbon chains with respect to bilayer normal. From x-ray diffraction pattern of highly oriented sample (Fig. 1.7), one can directly measure the tilt angle and also identify the tilt direction with respect to the chain lattice. Procedure to measure tilt angle will be discussed in chapter 2.

Different levels of hydration can be achieved by either changing the water content of the sample or fixing the relative humidity (RH) of the local environment. For aligned samples the latter procedure is used. Three different types of gel phases have been found to exist in DMPC at different levels of hydration [6, 7] (Fig. 1.8). At high hydration the $L_{\beta I}$ phase was seen, where the tilt angle is $\sim 32^\circ$ and the direction of the tilt is towards nearest neighbour. The $L_{\beta L}$ was found on partial hydration, where the direction of the tilt is arbitrary. $L_{\beta F}$ was observed at low RH. In this phase the tilt direction is towards next nearest neighbour. The tilt angle is found to decrease gradually with decreasing RH [7]. It is important to note that these gel phases could be unambiguously identified, since oriented multilayers were used. However, it is difficult to distinguish them from the diffraction patterns of unoriented

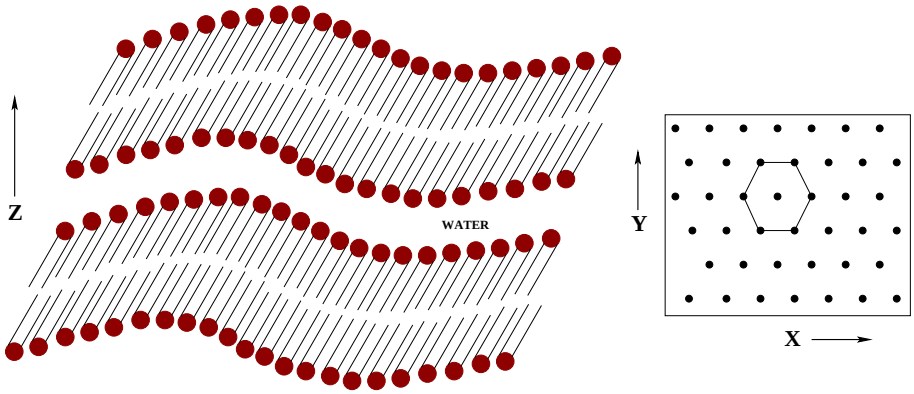

Figure 1.9: Schematic representation of the $P_{\beta'}$ phase.

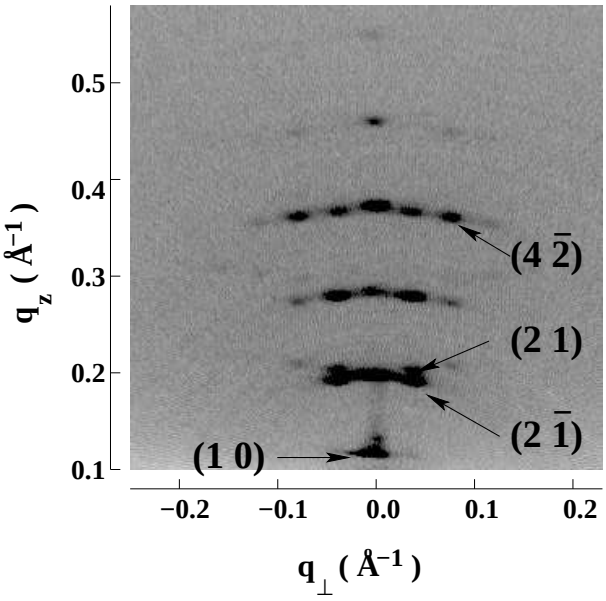

Figure 1.10: Diffraction pattern obtained from the $P_{\beta'}$ phase. The reflections can be indexed on an oblique lattice.

samples. Transitions among these gel phases were found to be continuous.

Many lipids which exhibit $L_{\beta'}$ phase show a ripple ($P_{\beta'}$) phase in between L_α and $L_{\beta'}$ at high hydration. The $P_{\beta'} \rightarrow L_{\beta'}$ transition is known as pre-transition. This transition is absent for lipids such as PE. This phase is characterized by a two dimensional oblique lattice formed by height modulated bilayers, as shown in Fig. 1.9. Typical diffraction pattern of the $P_{\beta'}$ phase is shown in Fig. 1.10. The wavelength of the modulation is $\sim$ 150 Å. In-plane hydrocarbon chain ordering is similar to that in the gel phase. Although hydrocarbon chains in both the $L_{\beta'}$ (L_β) and $P_{\beta'}$ are packed in a hexagonal lattice, head groups are not

ordered. Reducing the water content, or equivalently lowering RH, affects the main- and pre-transition temperatures. T_m goes up on decreasing RH. At sufficiently low RH pre-transition disappears (Fig. 1.8). Additives, such as cholesterol, can also affect or abolish the main- and pre-transitions of lipids.

Apart from these three phases, lipids exhibit another phase, known as the L_c phase, at temperatures below the gel phase. In general, the L_c phase occurs after long incubation at low temperatures, typically 4°C. L_c is a highly ordered phase where hydrocarbon chains as well as head groups are ordered.

1.3 Influence of cholesterol on lipid membranes

Cholesterol belongs to a class of polycyclic organic compounds known as sterols. It is an essential and ubiquitous component of animal tissues. Cholesterol is found in the membranes but the concentration of cholesterol is different in different membranes. The structure of cholesterol is shown in Fig 1.11. The presence of the hydrophilic *OH* group helps to orient cholesterol at the membrane–water interface of the bilayer. It can form a hydrogen bond with neighbouring lipid molecule especially with sphingomyelin. It is well known that cholesterol enhances the rigidity of the plasma membranes. It is also believed to be responsible for lateral organization of lipids in the membranes in sub-micrometer domains, called rafts, and is known to regulate the activities of certain membrane proteins [8].

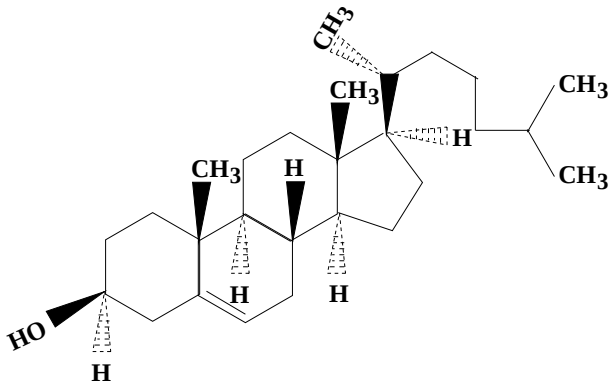

Figure 1.11: Structure of cholesterol

Table 1.2: Approximate lipid contents of different cell membranes [1].

lipids	liver plasma membrane	Erythrocyte plasma membrane	Myelin	Mitochondrion	Endoplasmic reticulum	*E. coli*
Cholesterol	17	23	22	3	6	0
PE	7	18	15	35	17	70
PC	24	17	10	39	40	0
PS	4	7	9	2	5	trace
Sphigomyelin	19	18	8	0	5	0
Glycolipids	7	3	28	trace	trace	0
Others	22	13	8	21	27	30

As discussed earlier, lipids and cholesterol are major and important constituents of the plasma membranes (see table 1.2). Therefore, it is important to understand the influence of cholesterol on membrane properties. Biological membranes are complex. Therefore, model membranes of lipid–cholesterol mixtures have been studied to gain useful information in order to understand the behaviour of complex membranes [8]. There are mainly four different types of samples of lipid–cholesterol mixtures which are used to study the effect of cholesterol on lipid membranes: oriented multilamellar stack of membranes separated by water, dispersion of multilamellar vesicles in aqueous solution, giant unilamellar vesicles, and monolayers. Experimental techniques, such as differential scanning calorimetry (DSC), spectroscopic techniques (nuclear magnetic resonance (NMR), electron spin resonance (ESR) and fluorescence), diffraction techniques (x-ray and neutron), microscopy (freeze fracture electron microscopy, fluorescence microscopy and atomic force microscopy), have been widely used to probe membrane characteristics in the presence of cholesterol.

The effect of cholesterol on the main- (T_m) and pre-transition (T_p) temperatures of lipid bilayers has been determined by DSC experiments. A progressive decrease in T_m, T_p, transition enthalpies and the broadening of DSC thermograms with increasing cholesterol concentration indicate that cholesterol transforms the gel phase into a fluid phase [9, 10]. On the basis of DSC studies, it has been suggested that the gel phase is stabilized for lipids of chain lengths < 17 (number of carbon atoms), whereas for longer chain lengths (> 18) the fluid phase is stabilized [10]. This is due to the mismatch between the length of cholesterol

molecule (~ 17 Å) and the length of the hydrocarbon chains of the lipid molecule. Thickness of the bilayer in the presence of cholesterol is also dependent on the chain length and the phase state of lipids, but the orientation and the width of the head groups region are not affected significantly by cholesterol. For example, bilayer thickness is increased in the gel phase of PC bilayers for chain length from 12 to 16 carbons, as cholesterol is known to remove the chain tilt. However, for longer chain lengths, the bilayer thickness is decreased in the gel phase [11]. Bilayer thickness in the L_α phase is also increased due to the increase in conformational order by the stretching of the hydrocarbon chains in the presence of cholesterol. However, at low cholesterol concentrations, this effect is not significant [12].

Cholesterol induces non-lamellar phases in lipids, such as PEs and unsaturated PCs [13, 14]. Cholesterol also facilitates the formation of the L_c phase in PE bilayers [15] which in general occurs after long incubation at 4°C. In PCs, cholesterol strongly modifies the ripple wavelength (λ) of the $P_{\beta'}$ phase. λ increases with increasing cholesterol concentration and diverges at around 20 mol%, as revealed by freeze fracture and neutron scattering studies [16, 17].

Partial phase diagrams of lipid–cholesterol mixtures have been derived from various experimental techniques [17, 18, 19, 20, 21]. These studies suggest the coexistence of the gel ($L_{\beta'}/L_\beta$) with a cholesterol–rich phase, known as liquid ordered (l_o) phase below T_m. It is evident from the binary phase diagram obtained from diffraction study that cholesterol is miscible above T_m and there is no indication of macroscopic phase separation [17, 18]. However, spectroscopic studies, such as NMR and ESR, detect the coexistence of l_o with another fluid phase, known as liquid disordered (l_d) phase above T_m (Fig. 1.12 a) [19, 21]. At higher cholesterol concentrations typically > 20 mol%, the main transition completely disappears and the gel phase is replaced by the l_o phase. The l_o phase found at higher cholesterol content is thought to be relevant for biological membranes. The amount of cholesterol required to abolish the main transition and the maximum solubility of cholesterol are different for different lipids and depend on the nature of head group, chain saturation etc [22]. In general, cholesterol has greater affinity for saturated lipids than for unsaturated ones. This is due to

the fact that cholesterol cannot pack efficiently in the lipid bilayers if the molecules posses a *cis*-double bond, creating a kink in the chain. Among phospholipids, affinity for cholesterol increases in order of PC > PS >PE [9]. However, sphingomyelin has more affinity for cholesterol than PC [21]. This could be due to the ability of the -OH group of cholesterol to form hydrogen bond with the neighbouring sphingomyelin molecules. Lipid diffusion or mobility is decreased in the fluid phase and increased in the gel phase, as cholesterol concentration is increased, and it is found to be constant above 20 mol% [23]. For example, lateral diffusion constant in the fluid phase without cholesterol is $\sim 6.0 \times 10^{-12} m^2/s$, whereas with 50% cholesterol it decreases to $\sim 2.0 \times 10^{-12} m^2/s$. In the presence of cholesterol, conformational order in the L_α phase increases and hence molecular rotations about the bilayer normal become restricted. The orientional distribution function of lipid molecules gets narrowed down, indicating that most of the molecules are aligned parallel to the bilayer normal, which in turn increases the segmental order parameter of the chains [24]. The segmental order parameter in the presence of cholesterol in the L_α phase becomes approximately twice that in the pure system without cholesterol [21]. Increase in the bilayer bending rigidity ($\kappa \sim 10^{-19}$ J) in the presence of the cholesterol is a consequence of the increase in the orientional order in the fluid phase [25].

A thermodynamic model based on lipid–cholesterol interaction and acyl chain conformation has been used to calculate the phase diagram in binary lipid–cholesterol mixtures [26]. Two basic conformational states; an ordered state (all *trans*) and a disordered state, were used in the model. Entropic contribution comes from the conformational difference between the two states and from the ideal mixing of the states. Relative populations of the two conformational states were obtained by minimizing the free energy with respect to relative population subjected to the constraint that the sum of the two populations equals unity. The coexistence of two fluid (l_o and l_d) phases was obtained for reasonable range of values of model parameters. Introducing a solid phase with long range molecular packing within the bilayers, a temperature-concentration phase diagram has been determined. A microscopic model also provides a similar phase behaviour. In this model each monolayer is modeled

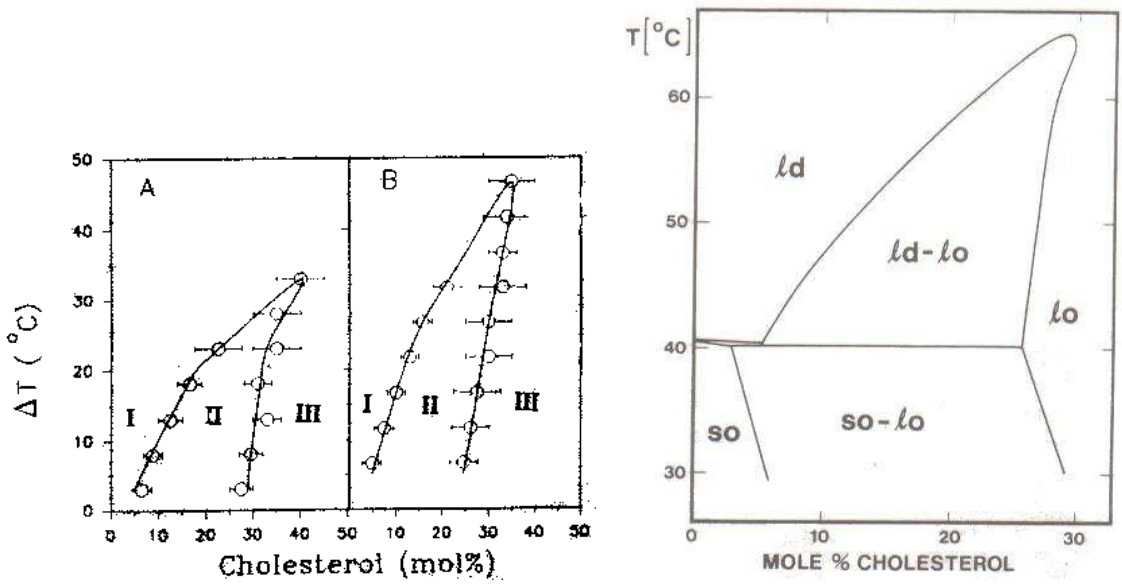

(a) (b)

Figure 1.12: (a) Partial phase diagram of binary mixtures of cholesterol with DPPC (A) and sphingomyelin (B) obtained from ESR study [21]. ΔT is the difference between the temperature of measurement and the corresponding main transition of pure lipid. I: l_d phase; II: $l_d + l_o$; III: l_o phase. (b) Theoretical phase diagram calculated from microscopic model [26].

as a triangular lattice where each lattice site is occupied either by acyl chain of the lipids or cholesterol. As in the case of the thermodynamic model, two conformational states, the ordered state and the disordered state, were considered for the acyl chains. Crystalline domains can develop in the plane of the bilayer with different orientations of the lattice. This is taken into account in the model by assigning a Potts variable to the PC molecules with ordered chain conformations. Hamiltonian for lipid-cholesterol mixtures was constructed by taking into account interaction energy between acyl chains and between acyl chain and cholesterol molecules using a mean field approximation. Minimizing the free energy derived from the Hamiltonian a phase diagram was obtained (Fig. 1.12 b) which is in agreement with the experimental phase diagram (Fig. 1.12 a) (see ref. [26] for details).

1.4 Membrane rafts

Plasma membranes are two dimensional fluids where the lipids can be considered as a solvent for membrane proteins [1]. Rafts are domains enriched with cholesterol and some specific membrane proteins such as glycosyl-phosphatidylinositol (GPI) anchored proteins that have been proposed to exist in cell membranes [27, 28] . They are believed to be involved in many cellular functions, such as endocytosis, protein trafficking and signal transduction. In spite of a large number of experimental studies to understand the organization of rafts, their existence and their intrinsic size have been poorly established. The only indirect evidence in support of rafts is the formation of detergent resistant membranes (DRM). DRM are the insoluble fraction of the membranes when they are dissolved in a solution of a detergent, such as Triton X-100, at 4°C. However, membranes are completely dissolved if the detergent solution is added at a high temperature (typically 37°C). Compositional analysis suggests that the DRM contains sphingolipids, cholesterol and GPI anchored proteins, which are believed to be the components of rafts. This is also further supported by the fact that cholesterol depletion using methyl-β-cyclodextrin reduces the amount of DRM. However, recent model membrane studies by Heerklotz showed that the detergent may induce domains on the lipid membranes [29]. Therefore, pre-existence of rafts before the addition of detergent cannot be conclusively inferred from the DRM.

Some experiments indicate that the intrinsic size of the membrane rafts is < 100 nm which is beyond the resolution of light microscopy. Lipid aggregates made up of sphingolipid–cholesterol condensed complexes (diameter ~ 7 nm) surrounding individual proteins are proposed to exist as mobile entities in the plane of the membranes. These lipid shells are targeted to preexisting lipid domains like caveolae/rafts which can bud off to transport their cargo to a specific location in the cell [30]. Diffusion of beads coupled by antibodies to lipids and GPI anchored proteins, and homo-FRET between GPI anchored proteins suggest that there are tiny lipid domains containing a few GPI anchored proteins present on the cell surface. However, these tiny domains may coalesce to form large scale structures

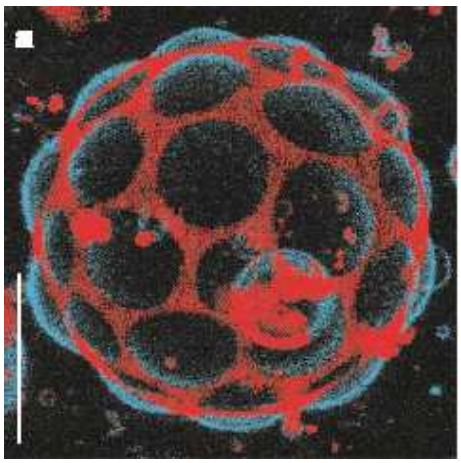

Figure 1.13: Micrograph of GUVs, showing coexistence of the l_o and l_d phases [35]. Scale bar, 5 μm.

under certain conditions [31, 32].

Model membranes composed of ternary mixtures of a saturated lipid (Sphingolipid, DPPC, DMPC etc), an unsaturated lipid (DOPC, POPC etc) and cholesterol have been widely used to mimic the behaviour of biomembranes [33, 34]. The coexistence of two fluid phases referred to as the l_o and l_d, seen in these systems below T_m of the saturated lipid, is believed to be relevant for the formation of rafts in plasma membranes. Giant unilamellar vesicles (GUVs) made up of ternary mixtures show micron sized domains of the l_o phase rich in the saturated lipid dispersed in the l_d phase (Fig. 1.13) [34, 35]. Differential partitioning of a fluorescent dye into the two fluid phases creates contrast between them and makes it possible to visualize the phase separation using fluorescence microscopy. The lateral diffusion and rotational motion of lipid molecules in the l_o phase is 2-3 times slower compared to those in the l_d phase, implying that the former phase has higher chain conformational order than the latter. The uniform fluorescence intensity on the surface of GUVs at higher temperatures (above T_m) suggests that the l_o and l_d phases are miscible, indicating no macroscopic phase separation. However, the possibility of some nanometer sized domains cannot be ruled out [19]. The fluid–fluid immiscibility is also seen in monolayers made from lipid–cholesterol mixtures. One of the fluid phases is proposed to be a condensed complex of lipid and cholesterol [36].

The complexity of the plasma membranes arises from the diversity of lipids and proteins present in them. Various active processes occurring on the cell surface make the situation even more complicated. It is important to note that the coexistence of two fluid phases seen in model membranes is an equilibrium phenomenon. However, it is not clear from the present literature whether the domains that are proposed in plasma membranes are equilibrium structures or maintained by some active processes. Therefore, we cannot rule out the possibility that the analogy between membrane rafts and domains in model membranes containing cholesterol is rather inappropriate. However, there are some aspects of lipid–cholesterol interactions that are not well understood even in model systems. Therefore, it is important to study the behaviour of these simpler systems in order to gain a better understanding of the much more complex biological membranes.

Bibliography

[1] B. Alberts, D. Bray, J. Lewis, M. Raff, K. Roberts, and J. D. Watson, *Molecular Biology of the Cell* (Garland publishing, Tayor and Francis Group, 1994).

[2] J. N. Israelachvili, *Intermolecular and Surface Forces,* (Academic Press, London, 1991).

[3] W. M. Gelbart, A. Ben-Shaul, and D. Roux, ed. *Micelles, Membranes, Microemulsions, and Monolayers* (Springer Verlag, New York, 1994).

[4] R. Lipowsky and E. Sackmann, ed. *Handbook of Biological Physics* (Volume 1, Elsevier Science B. V, 1995).

[5] R. Koynova and M. Caffrey, Biochim. Biophys. Acta **1376**, 91 (1998).

[6] G. S. Smith, E. B. Sirota, C. R. Safinya, R. J. Plano, and N. A. Clark, J. Chem. Phys. **92**, 4519 (1990).

[7] S. Tristram-Nagle, Y. Liu, J. Legleiter, and J. F. Nagle, Biophys. J. **83**, 3324 (2002).

[8] L. Finegold, ed. *Cholesterol in Membrane Models* (CRC press, Boca Raton, FL, 1993).

[9] T. P. W. McMullen and R. N. McElhaney, Biochemistry **36**, 4979 (1997).

[10] T. P. W. McMullen, R. N. A. H. Lewis, and R. N. McElhaney, Biochemistry **32**, 516 (1993).

[11] T. J. McIntosh, Biochim. Biophys. Acta **513**, 43 (1978).

[12] S. W. Hui and N. B. He, Biochemistry **22**, 1159 (1983).

[13] R. M. Epand, D. W. Hughes, B. G. Sayer, N. Borochov, D. Bach, and E. Wachtel, Biochim. Biophys. Acta **1616**, 196 (2003).

[14] H. Takahashi, K. Sinoda, and I. Hatta, Biochim. Biophys. Acta **1289**, 209 (1996).

[15] T. P. W. McMullen, R. N. A. H. Lewis, and R. N. McElhaney, Biochim. Biophys. Acta **1416**, 119 (1999).

[16] B. R. Copeland and H. M. McConnell, Biochim. Biophys. Acta **599**, 95 (1980).

[17] K. Mortensen, W. Pfeiffer, E. Sackmann, and W. Knoll, Biochim. Biophys. Acta **945**, 221 (1988).

[18] R. P. Rand, V. A. Parsegian, J. A. C. Henry, L. J. Lis, and M. McAlister, Can. J. Biochem. **58**, 959 (1980).

[19] M. R. Vist and J. H. Davis, Biochemistry **29**, 451 (1990).

[20] C. Paŕe and M. Lafleur, Biophys. J. **74**, 899 (1998).

[21] M. B. Sankaram and T. E. Thompson, Biochemistry **29**, 10670 (1990).

[22] J. Huang, J. T. Buboltz, and G. W. Feigenson, Biochim. Biophys. Acta **1417**, 89 (1999).

[23] A. Filippov, G. Orädd, and G. Lindblom, Biophys. J. **84**, 3079 (2003).

[24] G. Deinum, H. van. Langen, G. van. Ginkel, and Y. K. Levine, Biochemistry **27**, 852 (1988).

[25] D. Needham and R. S. Nunn, Biophys. J. **58**, 997 (1990).

[26] J. H. Ipsen, G. Karlström, O. G. Mouritsen, H. Wennerström, and M. J. Zuckermann, Biochim. Biophys. Acta **905**, 162 (1987).

[27] K. Simons and W. L. C. Vaz, Annu. Rev. Biophys. Biomol. Struct. **33**, 269 (2004).

[28] M. Edidin, Annu. Rev. Biophys. Biomol. Struct. **32**, 257 (2003).

[29] H. Heerklotz, Biophys. J. **83**, 2693 (2002).

[30] R. G. W. Anderson and K. Jacobson, Science **296**, 1821 (2002).

[31] W. K. Subczynski and A. Kusumi, Biochim. Biophys. Acta **1610**, 231 (2003).

[32] P. Sharma, R. Varma, Sarasij RC, K. G. Ira, G. Krishnamurthy, M. Rao, and S. Mayor, Cell **116**, 577 (2004).

[33] R. F. M. de Almeida, A. Fedorov, and M. Prieto, Biophys. J. **85**, 2406 (2003).

[34] S. L. Veatch and S. L Keller, Biophys. J. **85**, 3074 (2003).

[35] T. Baumgart, S. T. Hess, and W. W. Webb, Nature **425**, 821 (2003).

[36] H. M. McConnell and M. Vrljic, Annu. Rev. Biophys. Biomol. Struct. **32**, 469 (2003).